Low-frequency SST and upper-ocean heat content variability in the North Atlantic

Martha W. Buckley and Rui M. Ponte (Atmospheric and Environmental Research) and Gaël Forget and Patrick Heimbach (Massachusetts Institute of Technology)

Motivation

- **Observations indicate Atlantic SSTs exhibit significant low-frequency variability** (Bjerknes 1964; Kushnir 1994; Ting et al. 2009).
  - e.g. Atlantic Multidecadal Oscillation (Kerr, 2000; Knight et al., 2005)
- **The origin of Atlantic SST anomalies remains to be quantified.**
- Likely depends on **timescale**
  - Intra-annual to inter-annual: response to local atmospheric forcing (Frankignoul and Hasselmann, 1977), e.g. the NAO tripole (Cayan, 1992).
  - Longer timescales (how long?) ocean circulation may play a role.
- **Ocean dynamics that are important have not been isolated**
  - Wind and/or buoyancy forced baroclinic Rossby waves (Sturges et al 1998).
  - Large scale changes in Atlantic ocean heat transport due to changes in the AMOC (Kushnir 1994, etc.) and gyre circulations.
  - Lozier (2010): most significant question concerning the AMOC is role of AMOC in creating decadal SST anomalies.

Question

What are the relative roles of atmospheric forcing and ocean dynamics in setting upper-ocean heat content variability in the North Atlantic?

ECCO version 4 state estimate (1992-2010)

- MITgcm least squares fit to observations using adjoint (Wunsch et al., 2009)
- fit achieved by adjusting initial conditions, forcing, and model parameters
- well-suited to understand UOHC variability because it satisfies equations of motion and preserves property budgets exactly (Wunsch and Heimbach, 2013) .
- Atmospheric forcing: ERA-Interim
- Ocean data:
  - In-situ: Argo, CTDs, XBTs, mooring arrays
  - Satellite: AVHRR & AMSR-E SST, altimetry
- Model Details (G. Forget)
  - New global grid (LLC90): includes Arctic, 50 vertical levels with partial cells
  - Nominal 1° resolution with telescopic resolution to 1/3° near Equator
  - State of the art dynamic/thermodynamics sea ice model
  - Nonlinear free surface + real freshwater fluxes

Comparison to observations

Temperature Misfits

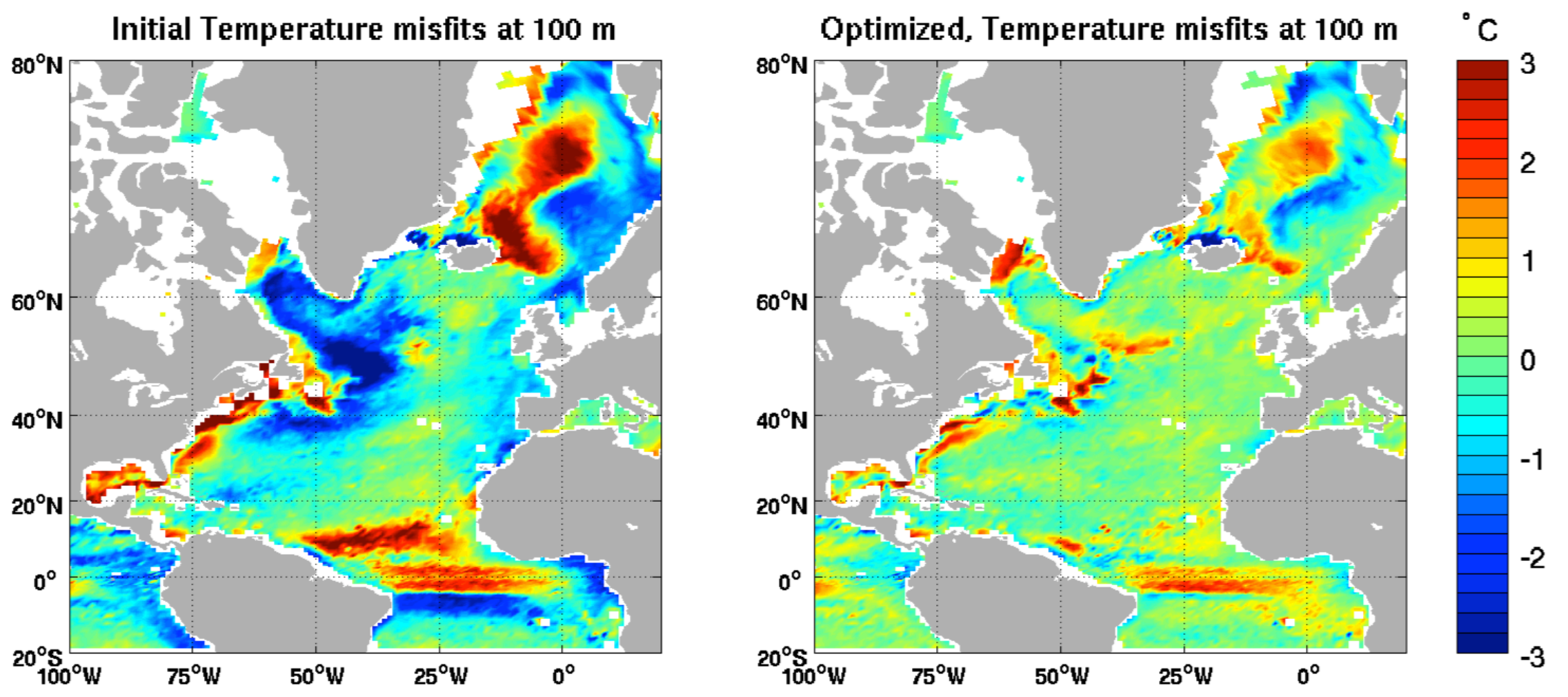

Temperature misfits for (left) "first-guess" solution and (right) optimized ECCO v4 solution at 100 m depth for all in-situ data (Argo, CTDs, XBTs, SeaOs) averaged over 1992-2010. Misfits are calculated as the sample mean for each grid cell of $T_e - T_o$, where T_o are observational profiles and T_e are the corresponding profiles from the model.

Comparison of observed and ECCO v4 SST variability

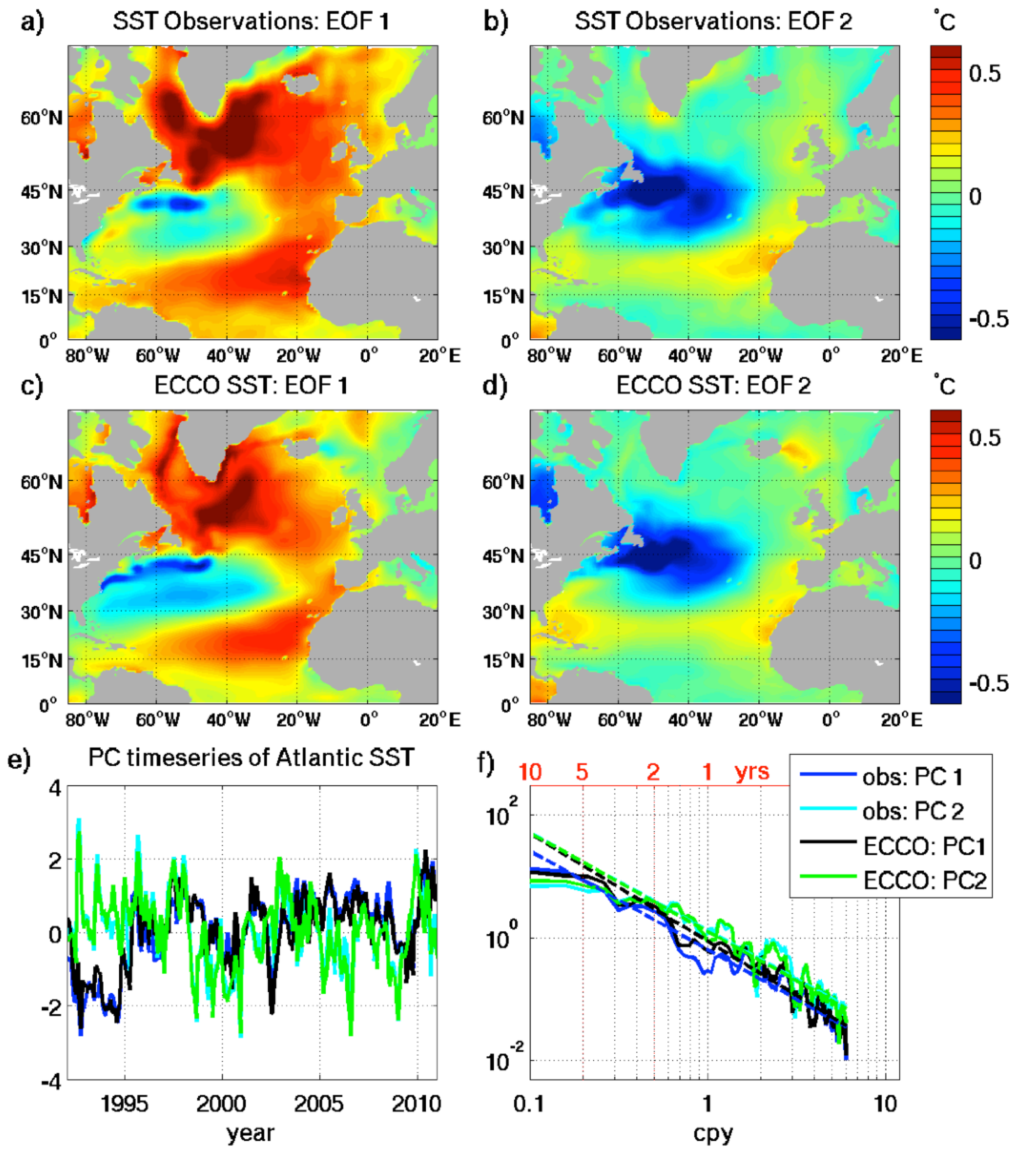

The first two empirical orthogonal functions (EOFs) of monthly (seasonal cycle removed) North Atlantic SST anomalies from (a-b) mapped Reynolds et al. (2002) data and (c-d) ECCO v4, which respectively explain ~25% and ~15% of the spatially integrated variance. (e) The first two principal component (PC) time series and (f) respective power spectra.

Upper-ocean heat content variability

Heat Content integrated over maximum climatological mixed layer depth (D)

- Measure of heat contained in "active" ocean layers.
- Relevant for understanding SST
- Avoids strong contributions from diffusion and eliminates entrainment effects (Deser et al, 2003; Coetlogon and Frankignoul, 2003; Buckley et al. 2014).
- Define: $H = \rho_o C_p \int_{-D}^{\eta} T\ dz$

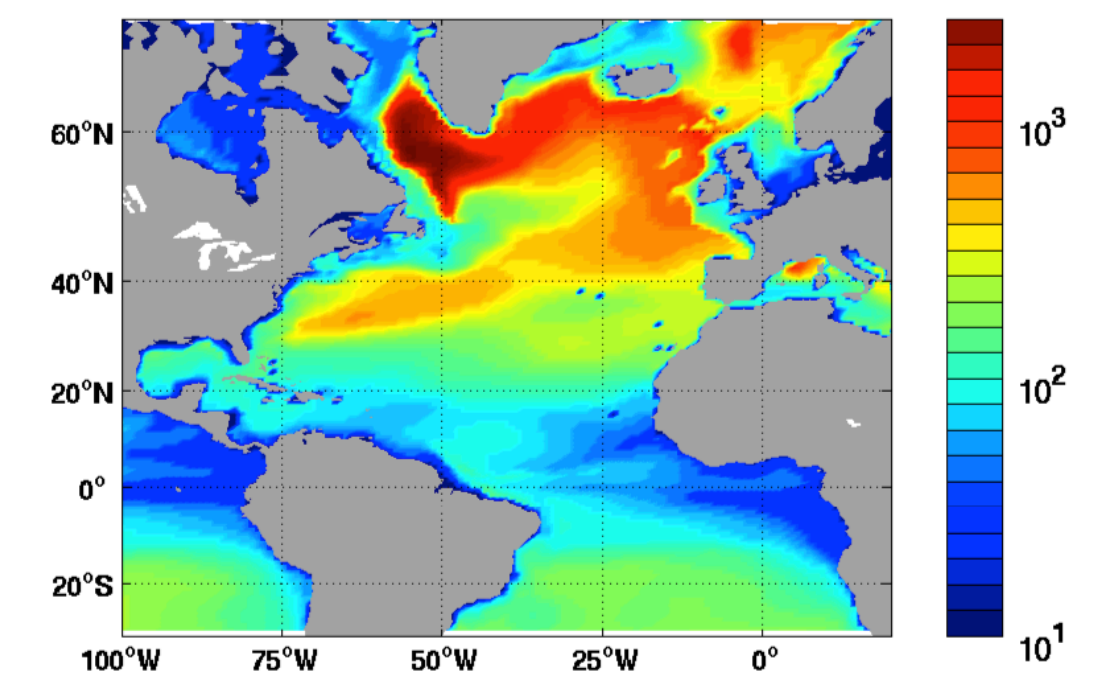

Maximum Climatological mixed layer depth (D)

To right:
(a) The first two PC time series of monthly H anomalies (seasonal cycle removed) over the North Atlantic and (b) their respective power spectra. EOF1 and EOF2 explain 50% and 11% of the variance, respectively.
(c-d) The first two EOFs of North Atlantic H.
(e-f) The spatial patterns of SST variability associated with the first two PC time series of North Atlantic H, obtained by projecting the PC time series onto monthly SST anomalies (seasonal cycle removed).

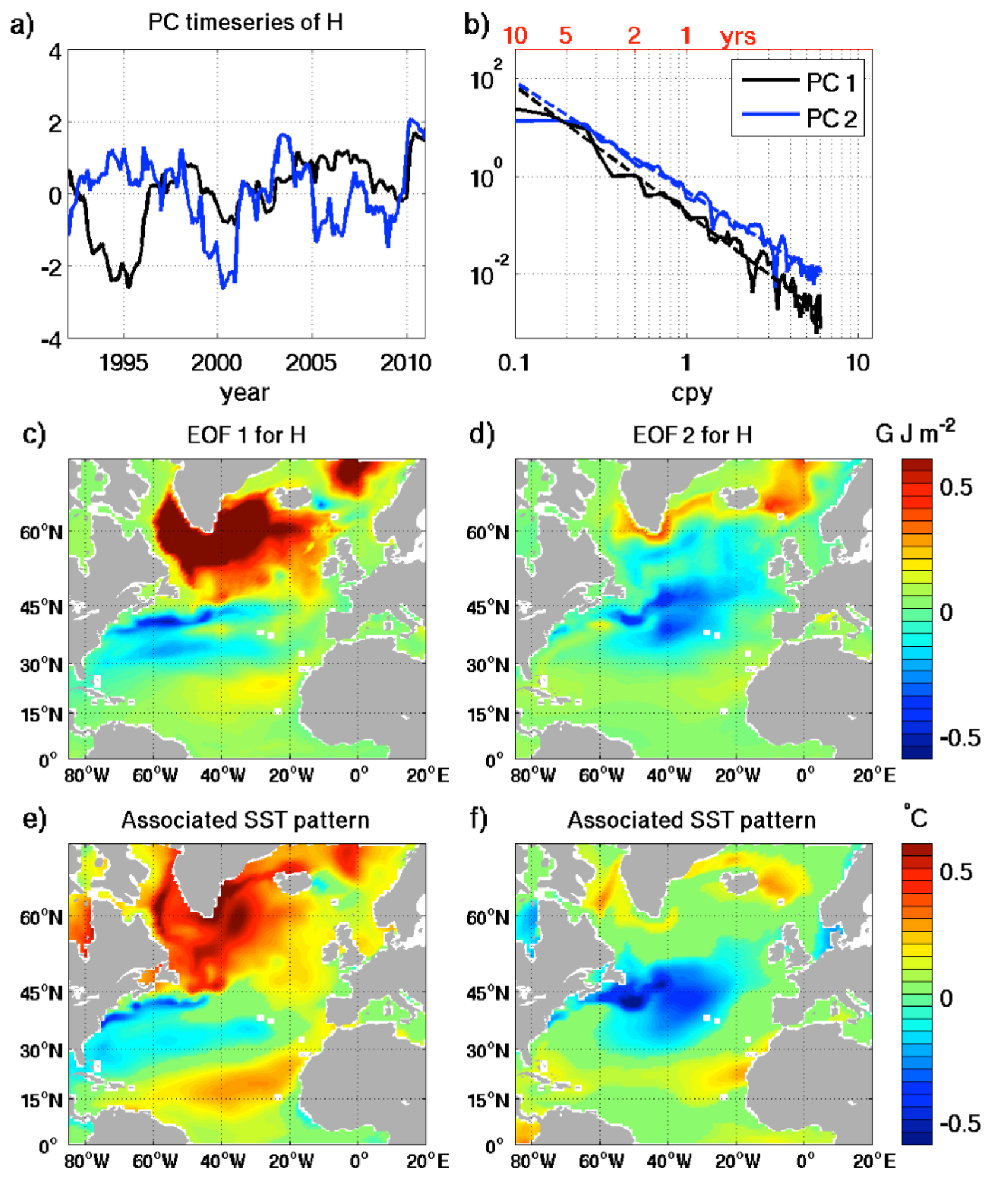

Heat content budgets

$$\underbrace{\rho_o C_p \int_{-D}^{\eta} \overline{\frac{\partial T}{\partial t}}\ dz}_{H_t} = \underbrace{-\rho_o C_p \int_{-D}^{\eta} \nabla\cdot(\overline{\mathbf{u}T} + \overline{\mathbf{u}^*T})\ dz}_{C_{adv}} - \underbrace{\rho_o C_p \int_{-D}^{\eta} \overline{\nabla\cdot\mathbf{K}}\ dz}_{C_{diff}} + \overline{Q}_{net}$$

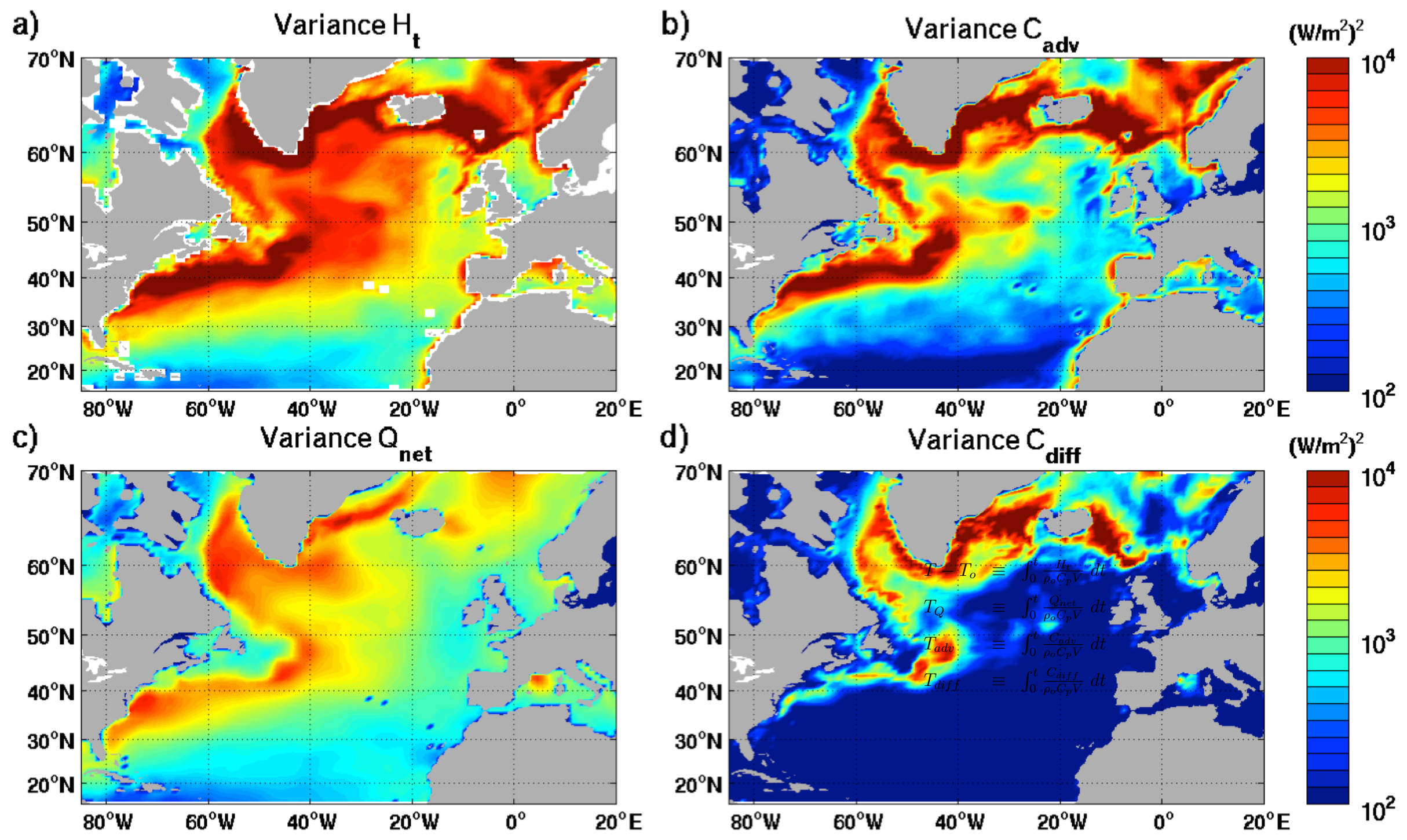

Variance of monthly anomalies (seasonal cycle removed) of terms in the H budget. (a) tendency H_t, (b) advective convergence C_{adv}, (c) air-sea heat flux Q_{net} and (d) diffusive convergence C_{diff}.

Advective convergences play a large role in H_t budget in areas of strong currents/fronts, such as along the Gulf Stream path.

Dynamics of Advective heat transport convergences

$$C_{adv} = \underbrace{-\rho_o C_p \int_{-D}^{\eta} \nabla\cdot(\bar{\mathbf{u}}\bar{T})\ dz}_{\text{linear: } C_{lin}} \underbrace{-\rho_o C_p \int_{-D}^{\eta} \nabla\cdot(\overline{\mathbf{u}'T'} + \overline{\mathbf{u}^*T})\ dz}_{\text{bolus: } C_{bol}}$$

$$C_{ek} = \rho_o C_p \int_{-D_{ek}}^{\eta} \nabla\cdot(\bar{\mathbf{u}}_{\mathbf{ek}}\bar{T})\ dz + \rho_o C_p\ \overline{w}_{ek}(-D)\ \overline{T}(-D)$$

$$C_g = \rho_o C_p \int_{-D}^{\eta} \nabla\cdot(\bar{\mathbf{u}}_{\mathbf{g}}\bar{T})\ dz + \rho_o C_p\ \overline{w}_g(-D)\ \overline{T}(-D)$$

- ū, etc. are monthly means.
- u' etc. are deviations from monthly means.
- u* is the eddy induced transport velocity parameterized by the Gent and McWilliams (1990) scheme.
- u_{ek} and u_g are the Ekman and geostrophic velocities.
- w_{ek} and w_g are calculated from u_{ek} and u_g according to the continuity equation.

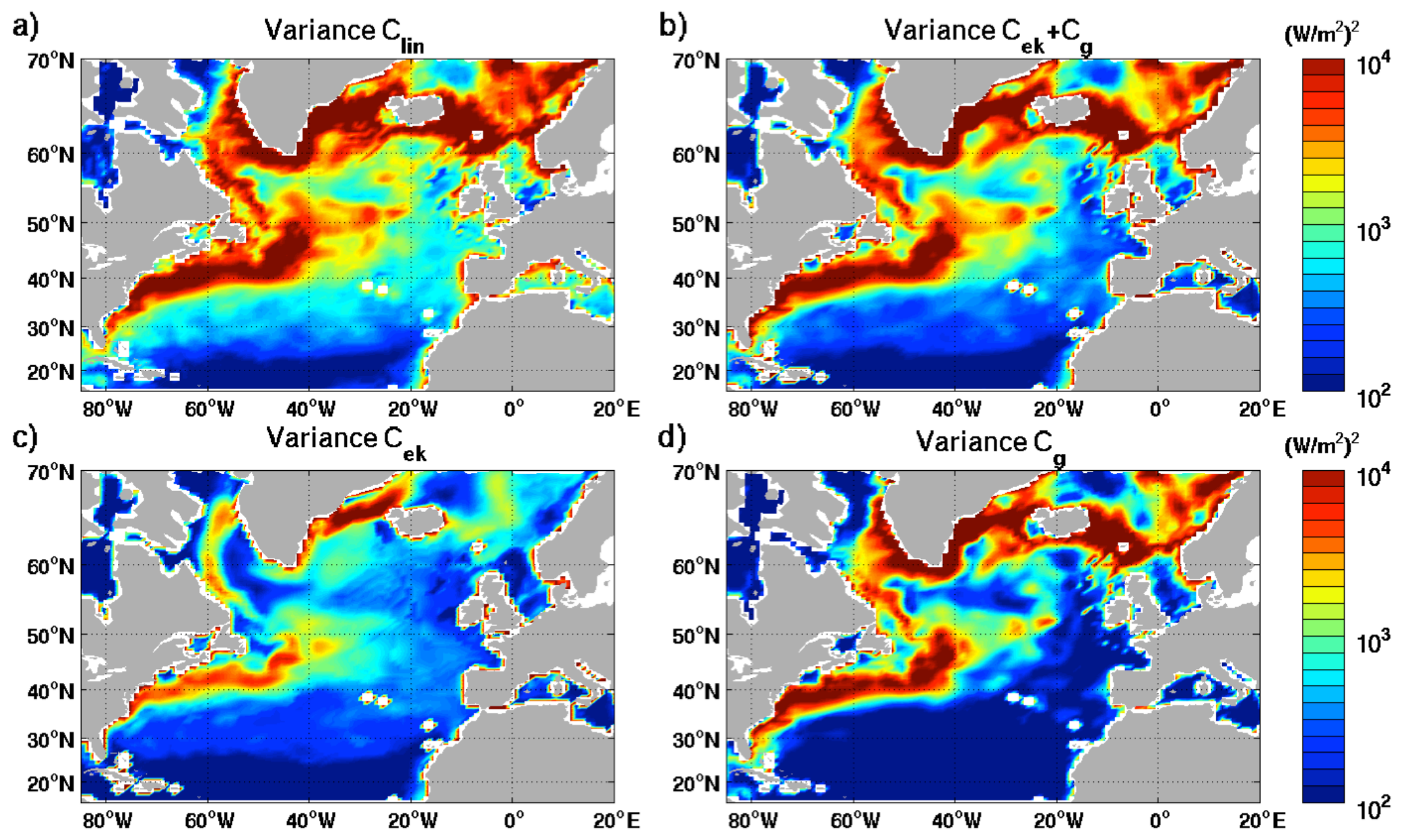

- Variance of C_{lin} and $C_{ek}+C_g$ similar to that of C_{adv} in most regions.
- Both C_{ek} and C_g are largest in regions of strong currents/ fronts.
- C_{ek} also plays a role in gyre interiors.

Variance of monthly anomalies of components of advective convergence C_{adv}: a) linear C_{lin}, b) estimated $C_{ek+}C_g$, c) Ekman C_{ek}, and d) geostrophic C_g.

Role of velocity variability, temperature variability, and their covariability

$$C_{ek}(\mathbf{u_{ek}}, w_{ek}, T) = C_{ek}(\bar{\mathbf{u}}_{\mathbf{ek}}, \overline{w}_{ek}, \overline{T}) + \underbrace{C_{ek}(\mathbf{u_{ek}}', w'_{ek}, \overline{T})}_{C^{v}_{ek}} + \underbrace{C_{ek}(\bar{\mathbf{u}}_{\mathbf{ek}}, \overline{w}_{ek}, T')}_{C^{T}_{ek}} + \underbrace{C_{ek}(\mathbf{u}'_{\mathbf{ek}}, w'_{ek}, T')}_{C^{vT}_{ek}}$$

- Overbars are averages over ENTIRE 19-year ECCO estimate
- Primes are deviations from these averages

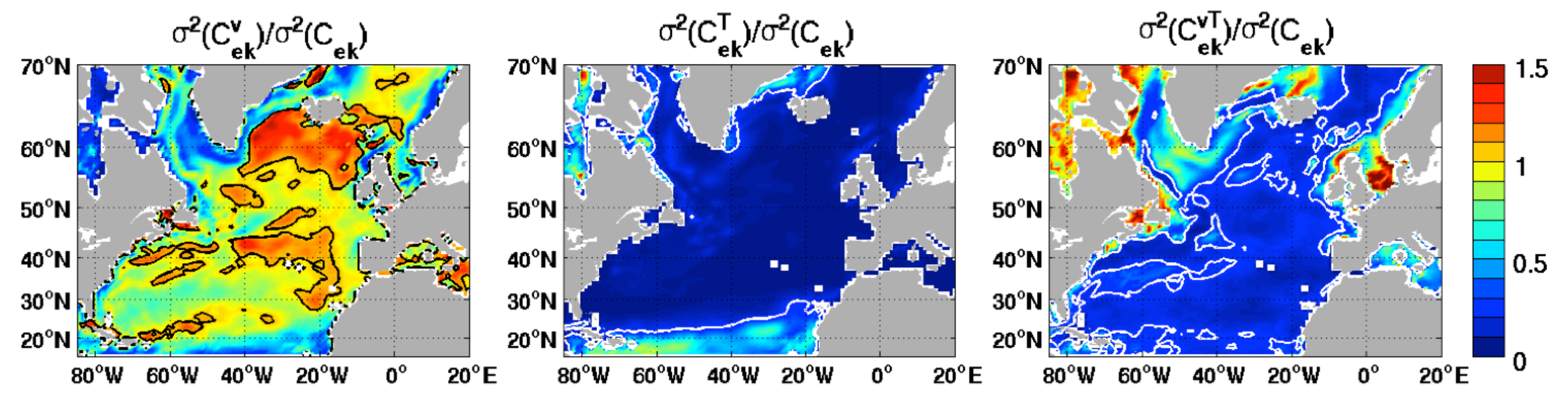

Variance of Ekman heat transport convergences due to velocity variability (C_{ek}^{v}) , temperature variability (C_{ek}^{T}), and their covariability (C_{ek}^{vT}) normalized by the variance of C_{ek}. Buckley et al. (submitted to *J. Climate*).

C_{ek}^{v} dominates the variability of C_{ek} except in the tropics, where C_{ek}^{T} is important and in the Labrador Sea where C_{ek}^{VT} plays a role.

Role of local atmospheric forcing

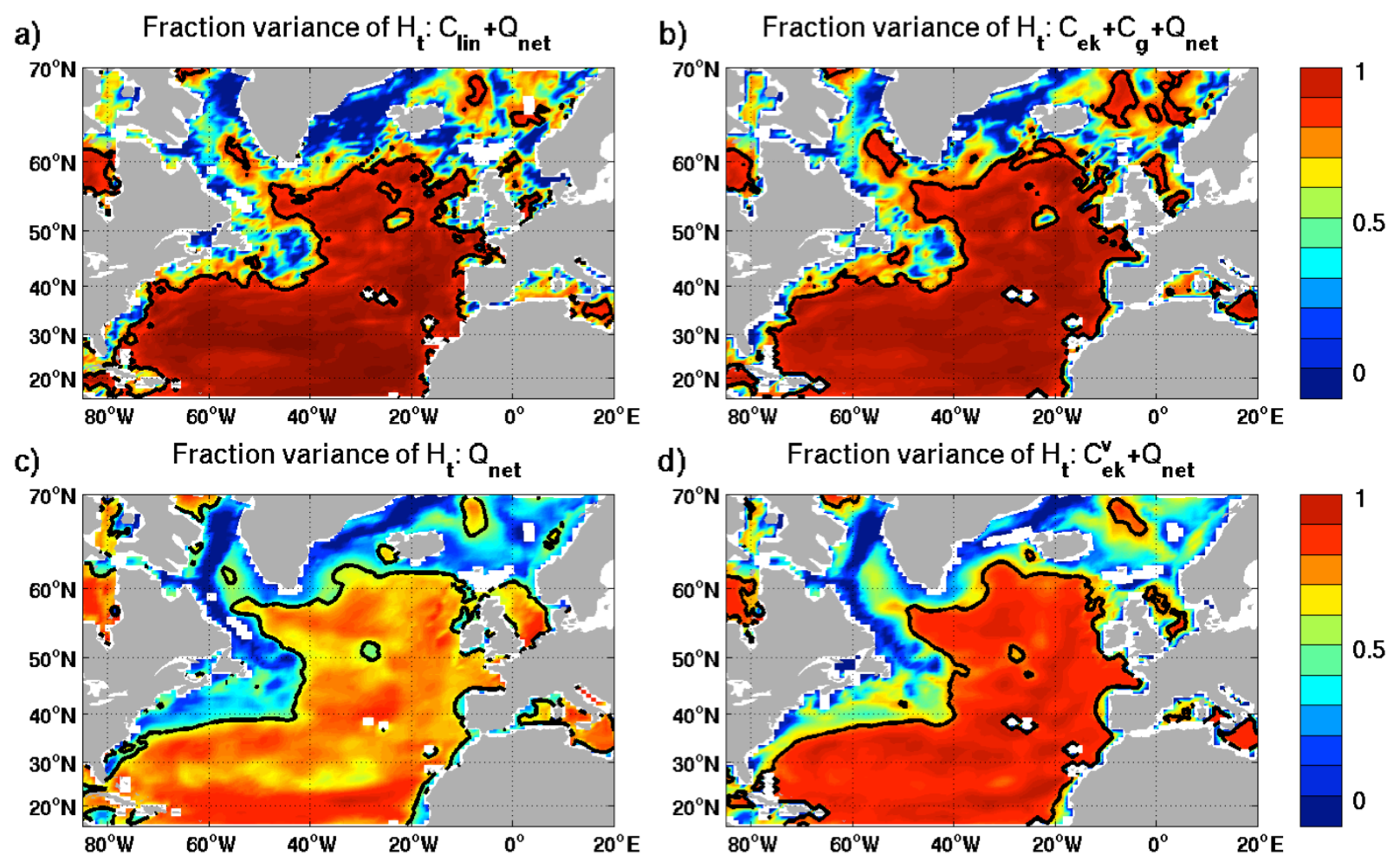

- Variance of H_t is well explained by $Q_{net}+C_{lin}$ or $Q_{net}+C_{ek}+C_g$ in most regions.
- In gyre interiors, 70% of variance of H_t explained by $C_{ek}^{v}+Q_{net}$, whereas Q_{net} alone only explains 50%.
- Geostrophic convergences important along Gulf Stream path

Maps showing the fraction of the variance of H_t explained by a) $C_{lin}+Q_{net}$ b) $C_{ek}+C_g+Q_{net}$, c) Q_{net} , and d) $C_{loc}^{*}=C_{ek}^{v}+Q_{net}$.

Hypothesis: $C_{ek}^{v}+Q_{net}= C_{loc}^{*}$ is a measure of impact of local atmospheric forcing on H

Regional Budgets

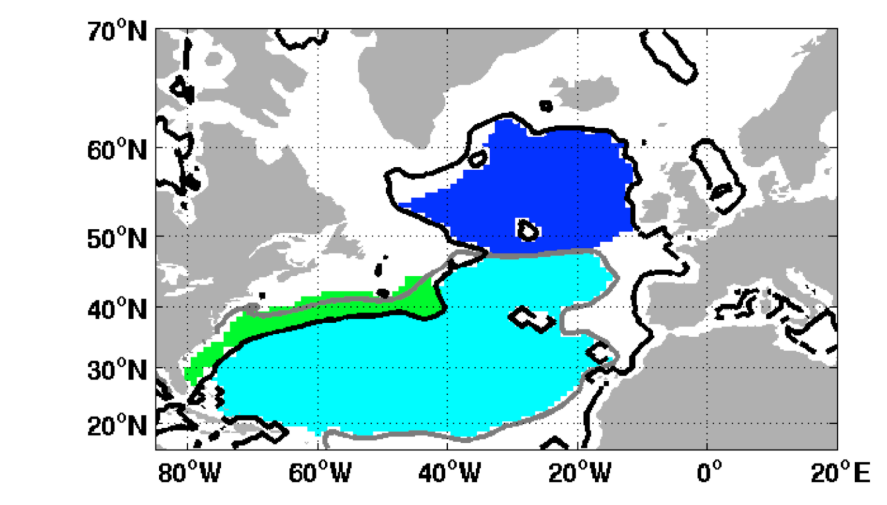

Temporally integrate:

$$T - T_o \equiv \int_0^t \frac{H_t}{\rho_o C_p V}\ dt \qquad T_{ek} \equiv \int_0^t \frac{C_{ek}}{\rho_o C_p V}\ dt$$

$$T_Q \equiv \int_0^t \frac{Q_{net}}{\rho_o C_p V}\ dt \qquad T_g \equiv \int_0^t \frac{C_g}{\rho_o C_p V}\ dt$$

$$T_{adv} \equiv \int_0^t \frac{C_{adv}}{\rho_o C_p V}\ dt \qquad T_{bol} \equiv \int_0^t \frac{C_{bol}}{\rho_o C_p V}\ dt$$

$$T_{diff} \equiv \int_0^t \frac{C_{diff}}{\rho_o C_p V}\ dt \qquad T_{loc} \equiv T_{air-sea} + T_{ek}$$

$$T_{loc} \equiv T_{air-sea} + T_{ek}^{v}$$

Coherences of H_t and fluxes

Time series of budget for H

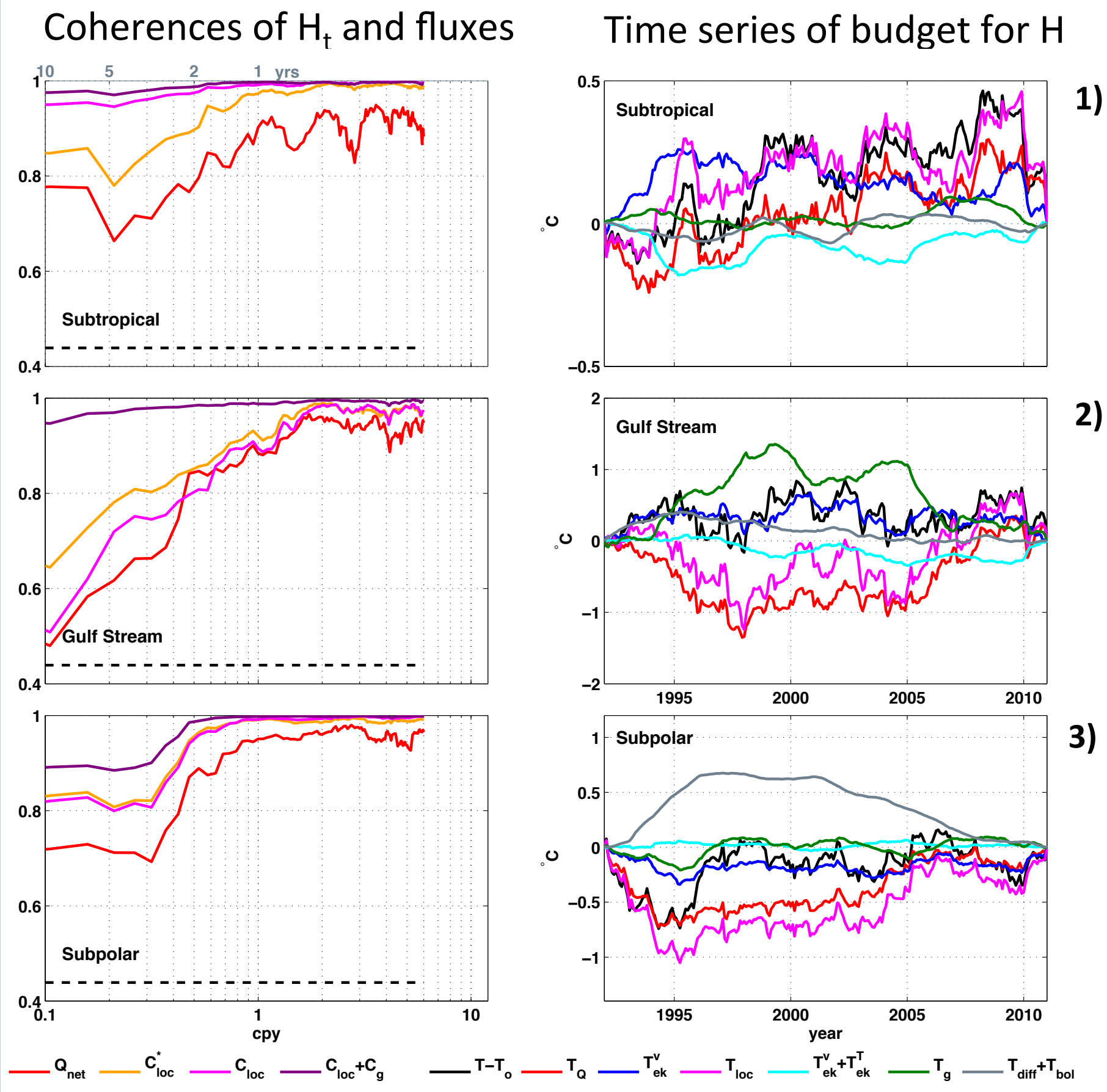

1) Subtropical gyre interior

- C_g, C_{diff}, C_{bol} negligible => $C_{loc}=C_{ek}+Q_{net}$
- C_{loc} dominates on all timescales
- T_{loc} explains 92% of the variance of H

2) Gulf Stream region

- C_{loc} dominates for τ < 6 mo
- C_g role for τ > 6 mo.
- T_g and T_Q highly anticorrelated
- H anomalies formed by C_g, damped by Q_{net}

3) Subpolar gyre

- C_{loc} dominates for τ < 1 yr.
- C_g, C_{diff}, C_{bol} play a role for τ >1 yr.

(left panels) coherence magnitude between H_t and Q_{net}, C_{loc}^{*}, C_{loc}, and $C_{loc}+C_{g.}$ (right panels) Time series for temporally integrated budgets for (top) the subtropical gyre, (middle) the Gulf Stream region and (bottom) the subpolar gyre.

Conclusions

- We utilize a dynamically consistent ocean state estimate (ECCO) to quantify the upper-ocean heat budget in the North Atlantic on monthly to interannual timescales.
- We introduce 3 novel techniques:
  - Heat content is integrated over the maximum climatological mixed layer depth (integral donated as H).
  - Advective heat transports are separated into Ekman and geostrophic parts, a technique which is successful away from boundary regions.
  - Air-sea heat fluxes and Ekman heat transport convergences due to velocity variability are combined into one "local forcing" term.
- Over most regions, variability of Ekman heat transport convergences is dominated by variability in the velocity field.
- Over broad swaths of the North Atlantic, including the interiors of the subtropical and subpolar gyres, >70% of the variance of H_t can be explained by local air-sea heat flux + Ekman transport variability.
- Geostrophic convergences play a role along Gulf Stream Path.
- North Atlantic separated into regions based on underlying dynamics and budgets of H analyzed in detail.
  - Subtropical gyre
    - local forcing dominates on all timescales.
  - Gulf Stream
    - local forcing dominates for periods less than 6 months; geostrophic convergences increasingly important on longer timescales.
    - Geostrophic convergences are anticorrelated with air-sea heat fluxes, suggesting H variability is forced by geostrophic convergences and damped by air-sea fluxes.
  - Subpolar gyre:
    - local forcing dominates for periods less than 1 year
    - geostrophic transports, bolus transports, and diffusion play a role on longer timescales.

References

1. **Buckley, M.**, R. Ponte, G. Forget, and P. Heimbach (2014). Low-frequency SST and upper-ocean heat content variability in the North Atlantic. *J. Climate*, **27**, 4996—5018.
2. **Buckley, M.**, R. Ponte, G. Forget, and P. Heimbach . Determining the origins of advective heat transport variability in the North Atlantic, submitted to *J. Climate*.
3. Bjerknes, J., 1964. Atlantic air-sea interaction. *Advances in Geophysics*, **10**, 1-82.
4. Cayan, D. R., 1992. Latent & sensible heat flux anomalies over the northern oceans: Driving sea surface temperature. *J. Phys. Oceanogr*., **22**, 859--881.
5. Deser, C., M. A. Alexander, and M. S. Timlin, 2003. Understanding the persistence of sea surface temperature anomalies in midlatitudes. *J. Climate*, **16**, 57–72.
6. de Coetlogon, G. and C. Frankignoul, 2003: The persistence of winter sea surface temperature in the North Atlantic. *J. Climate*, **16**, 1364–1377
7. Frankignoul, C., P. Muller, and E. Zorita, 1997. A simple model of the decadal response of the ocean to stochastic wind forcing. *J. Phys. Oceanogr*., **27**, 1533–1546
8. Kerr, R., 2000: A North Atlantic climate pacemaker for the centuries. *Science*, **288**, 1984–1986.
9. Knight, J. R., R. J. Allan, C. K. Folland, M. Vellinga, and M. E. Mann, 2005. A signature of persistent natural thermohaline circulation cycles in observed climate. *Geophys. Res. Lett.*, **32** (20).
10. Kushnir, Y., 1994. Interdecadal variations in North Atlantic sea surface temperatures and associated atmospheric conditions. *J. Climate*, **7**, 141-157.
11. Lozier, M.S., 2010. Deconstructing the conveyor belt. *Science*, **328**, 1507-1511.
12. Sturges, W., B.G. Hong, and A.J. Clarke, 1998, Decadal forcing of the North Atlantic subtropical gyre. *J. Phys. Oceanogr.*, **28**, 659-668.
13. Ting, Mingfang and Kushnir, Yochanan and Seager, Richard and Li, Cuihua. Forced and Internal Twentieth-Century SST Trends in the North Atlantic. *J. Climate*, **22**, 1469-1481.
14. Trenberth, K.E. and J.M. Caron, 2001: Estimates of meridional atmospheric and oceanic heat transports. *J. Climate*, **14**, 3433-3443.
15. Wunsch, C. and P. Heimbach, 2013: Dynamically and kinematically consistent global ocean circulation and ice state estimates. Ocean circulation and climate: observing and modeling the global ocean, G. Siedler, J. Church, J. Gould, and S. Gries, Eds., Elsevier, 2d ed.
16. Wunsch, C., P. Heimbach, R. M. Ponte, and I. Fukumori, 2009: The global general circulation of the ocean estimated by the ECCO consortium. *Oceanography*, **22**, 88–103.